Prediction Model of the Exit Cross Sectional Shape of Workpiece in Round-Oval-Round Pass Rolling

Youngseog Lee*
Plate, Rod & Welding Group at Technical Research Laboratories, Pohang Iron and Steel Corp. (POSCO), Pohang, P. O. Box 36 Korea
Byung-Min Kim, Dong Hwan Kim
School of Mechanical Engineering, Pusan National University, Pusan 609-735, Korea

A reliable analytic model that predicts the surface profile of the exit cross section of workpiece in round-oval (or oval-round) pass sequence is established. The presented model does not require any plasticity theory but needs the only geometric information on workpiece and roll groove. Formulation is based on the linear interpolation of the radius of curvature of an incoming workpiece and that of roll groove in the roll axis direction when the maximum spread of workpiece is known beforehand. The validity of the analytic model is examined by hot rod rolling experiment with the roll gap, specimen size, design parameter of oval groove and steel grade changed. Results revealed that the cross sectional shapes predicted by the model were in good agreement with those obtained experimentally. We found that the analytic model not only has simplicity and accuracy for practical usage but also saves a large amount of computational time in comparison with finite element method.

Key Words : Analytic Model, Surface Profile, Round Pass, Oval Pass, Rod Rolling

Nomenclature

A_h : Area fraction of workpiece above roll groove when the cross sections of workpiece and roll groove are overlapped.
A_s : Area fraction of workpiece cut out by B_c at the inside roll groove when the cross sections of workpiece and roll groove are overlapped.
B_c : Interval of two cross points in the roll axis direction when the cross sections of workpiece and roll groove are overlapped.
B_x : x-coordinate of cross point of surface profile and oval groove
B_y : y-coordinate of cross point of surface profile and oval groove
C_x : x-coordinate of cross point of workpiece and roll groove
C_y : y-coordinate of cross point of workpiece and roll groove
D_r : Roll depth
D_x : Distance between the center of round groove and that of surface profile
G : Roll gap
H_i : Maximum height of incoming workpiece
W_i : Maximum width of incoming workpiece
$\bar{H}_i$: Equivalent height of incoming workpiece
$\bar{H}_o$: Equivalent height of outgoing workpiece
H_p : Pass height
R_1 : Radius of curvature of oval groove
R_f : Radius of final surface profile of oval groove
R_g : Radius of curvature of round groove
R_{max} : Maximum radius of roll
R_{mean} : Mean radius of roll
R_s : Radius of surface profile of workpiece at a pass
W_f : Face width of oval groove

* Corresponding Author,
E-mail : pc554162@posco.co.kr
TEL : +82-54-220-6058; **FAX** : +82-54-220-6911
Plate, Rod & Welding Group at Technical Research Laboratories, Pohang Iron and Steel Corp. (POSCO), Pohang, P. O. Box 36 Korea. (Manuscript **Received** July 4, 2001; **Revised** November 28, 2002)

W_{max} : Maximum spread of workpiece at a pass
α : Relief angle of round groove
γ : Correction coefficient dependent on pass type

1. Introduction

In continuous hot rod (or bar) rolling process, billets are processed into rods (or bars) with acceptable dimensional tolerance as they pass through the rolling stands (passes), with the cross sectional shape being progressively altered. Thus, a precise prediction of the stress free surface profile of material (workpiece) that does not contact the roll directly is crucial in designing a rolling schedule and optimizing it. Stress free surface profile is referred to as surface profile hereafter for convenience. In addition, when we need to compute the thermo-mechanical parameters (strain, strain rate and temperature), which are necessary for predicting material's microstructural state (mean austenite grain size and recrystallized volume fraction, etc.), in average sense, during rolling we should first be able to predict the surface profile of the exit cross section because those parameters are directly dependent on it. This leads a process designer (or analyst) to focus on how to make a model for predicting the surface profile (i.e., cross sectional shape) of workpiece at a given pass over a range of rolling parameters.

In the past, the process designer relied on the empirical model based on tryout in mill yard test. These models were in conjunction with the formulae employed in plate rolling together with fitting constants on a basis of wide-ranged experimental data, which require high cost and a lot of time. These are well summarized in Ref. (Wusatowski, 1969). This type of model, however, most likely leaded to unsatisfactory results because it did not properly take into account the rolling parameters associated with rod (or bar) rolling.

Shinokura and Takai (1983) proposed an equation which predicts the maximum spread of an outgoing (exit) workpiece as a function of the roll radius, the geometry of an incoming (inlet) workpiece and the area fraction between the incoming workpiece and the geometry of roll groove. Then, they presented a model for predicting the surface profile of exit cross section in an oval pass rolling. The surface profile, however, was approximated as a curve consisting of two arcs. Hence, the surface profile was not smooth at the point of the maximum spread. Kemp (1990) proposed a deformation model to calculate the surface profile of a workpiece in an oval groove and a round groove rolling, and compared the predicted surface profile with the experimentally determined surface profile. Kemp (1990), however, did not present the equations used for the prediction of it.

Since 1990, a number of numerical studies on the basis of three-dimensional finite element analysis have been presented for predicting the surface profile of workpiece during rod (or bar) rolling (Park and Oh, 1990; Kim et al., 1992; Shin, et al., 1992; Komori, 1997; Kwon and Im, 1998; Kim and Im, 1998). FEA is very effective in predicting the cross sectional shape (surface profile) of workpiece but requires at least half an hour to run a program for a single pass since three dimensional analysis is required in nature. Thus, considering computational time for a number of passes in rod mill and complicated boundary conditions (friction coefficient on the roll/material interface and heat transfer coefficients dependent on the temperature and roll pressure), the capability for predicting the cross sectional shape by an analytic model, which is non-iterative in computation and is of reliable accuracy, has been highly desired.

In this study, an analytic model that predicts the cross sectional shape of workpiece in oval and round pass rolling sequences, which are most widely employed in rod (or bar) rolling process, is proposed. The cross sectional shape of an outgoing workpiece is predicted by using a weighting function and the linear interpolation of the radius of curvature of an incoming workpiece and that of roll groove in the roll axis direction when the maximum spread of it is known beforehand. The requirements placed on the choice of the weighting function were to ensure the spec-

ified boundary conditions.

The validity of the presented analytic model is examined by hot rod rolling experiment. A two-high laboratory mill with DCI (Ductile Casting Iron) roll of 310mm diameter was used. Experiment included the changes of i) roll gap (pass height), ii) diameter of incoming specimen, iii) design parameter of the oval groove, iv) ratio of roll diameter to specimen diameter and v) steel grades. The rolling temperature and friction conditions between workpiece and roll grooves were fixed. The cross sectional shapes of the workpiece measured at room temperature after each pass were compared with those calculated by the analytic model.

2. Problem Formulation

The formulation is based on the maximum spread formula (Shinokura and Takai, 1983) and the linear interpolation technique of the geometry of an incoming workpiece and that of roll groove in the roll axis direction.

2.1 Maximum spread model in oval-round (or round-oval) pass rolling

Shinokura and Takai (1983) carried out an experiment using a pilot hot rolling mill and developed the maximum spread formula for a mild steel (JIS SS41) in four types of passes, including Square-Oval, Round-Oval, Square-Diamond and Diamond-Diamond. The idea behind their formulae was that the maximum spread of an outgoing workpiece can be expressed as a function of the roll radius, the geometry of an incoming workpiece and the area fraction between the incoming workpiece and the geometry of roll groove. Figures 1 and 2 illustrate the definition of area fraction and equivalent heights in round-oval and oval-round pass rolling, for example. The equation for the maximum spread, W_{max}, was expressed as follows:

$$W_{max}=W_i\left[1+\gamma\frac{\sqrt{R_{mean}(\bar{H}_i-\bar{H}_o)}}{W_i+0.5H_i}\cdot\frac{A_h}{A_o}\right] \quad (1)$$

where

$$\bar{H}_o=\frac{A_o-A_s-A_h}{B_c} \text{ and } \bar{H}_i=\frac{A_o-A_s}{B_c} \quad (2)$$

W_i and H_i are, respectively, the maximum width

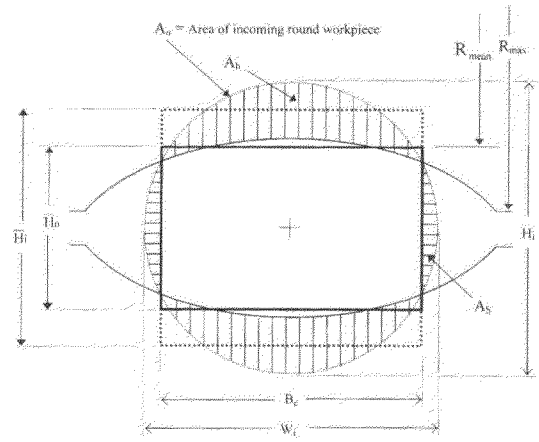

Fig. 1 Application of equivalent rectangle approximation to round-oval pass for calculating the effective height for workpiece and the area fraction between the incoming workpiece and the geometry of roll groove

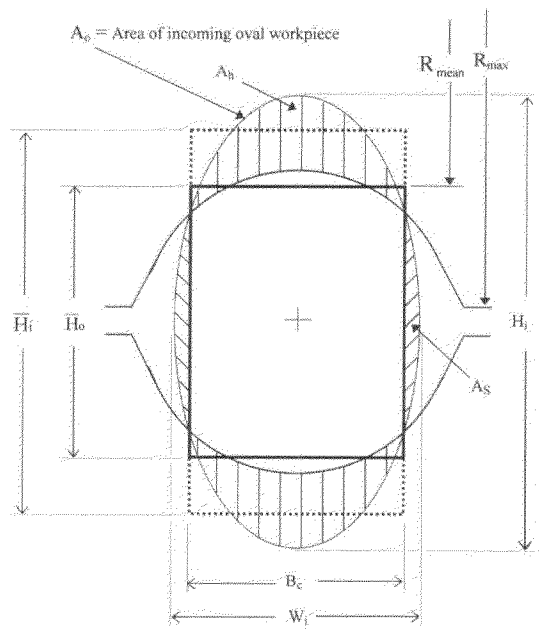

Fig. 2 Application of equivalent rectangle approximation to oval-round pass for calculating the effective height for workpiece and the area fraction between the incoming workpiece and the geometry of roll groove

and the maximum height of an incoming workpiece (i.e., inlet cross section) and γ is a coefficient dependent on pass type. This formula is of a very simple form and has only a coefficient but can predict the maximum spread with practical accuracy. Shinokura and Takai (1983) proposed that the common value of γ for all four passes was 0.83.

2.2 Surface profile in round-oval pass rolling

The schematic for the round-oval pass rolling is described in Fig. 3. When the incoming round workpiece is deformed at the inside of oval groove and at last reaches at the face width of oval groove, W_f, the final surface profile of the deformed workpiece is assumed to be a circle with radius of R_f. The R_f can be then approximated as a radius of a circle, which is located within the roll groove area and passes through the points ($x=\pm W_f/2$, $y=0$). R_a is the radius of curvature of the inlet cross section, R_s is the radius of curvature of the outlet cross section, and R_1 is the radius of the roll groove. Assuming that W_{max} does not exceed W_f (the width of the roll groove area), then R_s, is given as

$$R_s=R_a \cdot W_t+R_f \cdot (1-W_t) \tag{3}$$

$$\text{where } W_t=\frac{W_f-W_{max}}{W_f-W_1} \tag{4}$$

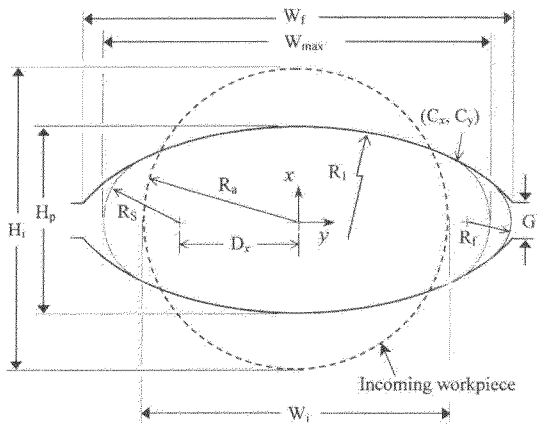

Fig. 3 Geometrical designation of roll groove, the incoming workpiece and the radius of surface profile, R_s, of the outgoing workpiece in round-oval pass rolling

W_t is a weighting function, W_1 is the width of the inlet cross section and W_{max} is the maximum spread of the exit cross section, which can be calculated by Eq. (1). The R_f is the radius to be achieved when $W_{max}=W_f$. The requirements placed on the choice of the weighting function stem from the need to ensure Eq. (3). According to Eqs. (3) and (4), R_s becomes R_a when $W_{max}=W_1$ (no spread at all), and R_s becomes R_f when $W_{max}=W_f$.

R_f, the radius of a circle located within the roll groove area is expressed in a form of

$$R_f=\frac{R_1H_p-(W_f^2+H_p^2)/4}{2R_1-W_f} \tag{5}$$

where H_p is the height of the roll groove. Derivation procedure for R_f is described in detail in Appendix. Once R_s is determined, the contact point (C_x, C_y) can be obtained. Then, the area of the exit cross section can be calculated from

$$A_{oval}=4\left[\int_0^{C_x}(R_1^2-x^2)^{1/2}dx-(R_1-H_p/2)C_x+\frac{\pi}{4}R_s^2-\int_0^{D_x}(R_s^2-x^2)^{1/2}dx\right] \tag{6}$$

$$\text{where } D_x=C_x-(W_{max}/2-R_s)$$

2.3 Surface profile in oval-round pass rolling

The geometrical designation of the oval-round pass rolling is described in Fig. 4. R_1 is the radius of curvature of the inlet cross section, and R_g is the radius of the round groove. Assume that the maximum spread, W_{max}, does not exceed W_f. Then, the radius of the surface profile, R_s, of the exit cross section is proposed as follows:

$$R_s=R_1 \cdot W_t+R_f \cdot (1-W_t) \tag{7}$$

$$\text{where } W_t=\frac{W_f-W_{max}}{W_f-W_1} \tag{8}$$

W_t is a weighting function, W_1 is the width of the inlet cross section and W_{max} is the maximum spread of the exit cross section, which can be calculated using Eq. (1). Note that, in the round pass, W_f is equal to $H_p(=2R_g)$. Then, the radius of the final surface profile, R_f, in Eq. (7) can be simply replaced by R_g and subsequently R_s can

be calculated. It should be noted that Eqs. (7) and (8) are valid under the condition that the maximum spread of the outgoing workpiece is not greater than round groove diameter, and $(D_r+G/2)$ is equal to R_g. If $(D_r+G/2)$ is not equal to R_g, the round roll groove is not a round shape any more.

Once R_s is determined, the contact point (C_x, C_y) can be obtained and the cross sectional area is computed as

$$A_{round}=4\int_0^{C_x}(R_g^2-x^2)^{1/2}dx+2R_s^2(2\theta-\sin 2\theta)$$

$$\text{where } \theta=\sin^{-1}(C_y/R_s) \tag{9}$$

It should be noted that the modeling concept employed in the round-oval pass rolling can be easily extended to the box-oval pass or initial billet-box pass rolling if the shape of incoming workpiece is replaced properly. In the case of the box-oval pass, the radius of curvature of the inlet cross section becomes infinite. This problem was overcome by assuming that it is twice the width of the inlet cross section. For the billet-box pass, the surface profile of the outgoing workpiece was assumed to be approximately a straight line rather than a curve. At the box pass, the material flow such as the maximum spread mainly influenced by the geometry of roll groove should be smaller than that affected by the geometry of oval and/or round grooves. Therefore, the coefficient, γ, affecting the maximum spread of workpiece in Eq. (1), might be less than 0.83, assigned for the oval pass and round pass.

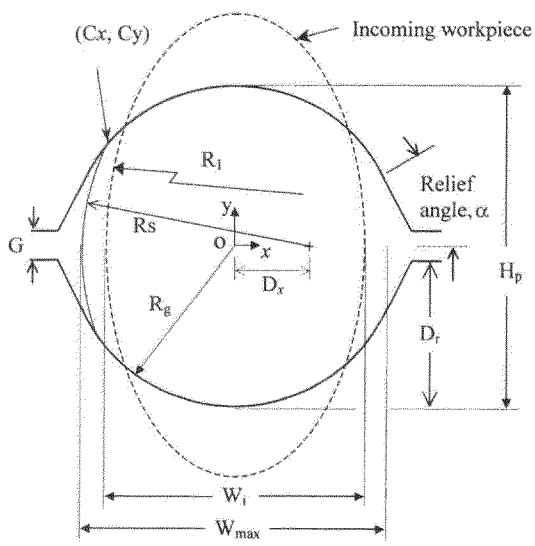

Fig. 4 Geometrical designation of roll groove, the incoming workpiece and the radius of surface profile, R_S, of the outgoing workpiece in oval-round pass rolling. The R_S on the right hand side is omitted for clarity

3. Experiment

3.1 Rolling equipment

A single stand two-high laboratory mill was employed, driven by 75kW constant torque DC motor. DCI rolls with 310mm in maximum diameter and 320mm in face width were used. The rolling speed was set at 34 rpm, which was equivalent to a rolling speed of 0.5m/s. A box type furnace with the maximum working temperature of 1400°C was employed to heat up the specimens to the desired rolling temperature.

3.2 Specimen preparation

Two plain carbon steels (S10C, SWRH72A) and two alloy steels (SAE9254, POSWELD2B) were used. The chemical composition of the steels used in the experiment is given in Table 1. The materials were obtained in the form of square that is, as-cast billet with a side length of 160mm. The specimens to be rolled were cut and machined into a round bar with 60mm in diameter and 300mm in length. To study the effect of the ratio of specimen size to work roll diameter, round bar specimens with 28mm in diameter and 300mm in length were also machined.

Table 1 Chemical composition (wt%) of the steels used in this study

S10C	Fe-0.10% C-0.25% Si-0.45% Mn-0.03% P-0.035% S
SWRH72A	Fe-0.72% C-0.25% Si-0.45% Mn-0.03% P-0.030% S
SAE9254	Fe-0.55% C-1.40% Si-0.70% Mn-0.035% P-0.04% S-0.7% Cr
POSWELD2B	Fe-0.05% C-0.825% Si-1.65% Mn-0.03% P-0.03% S-0.5% Cr-0.21% Ti-0.03% Zr

3.3 Experimental procedure

In order to measure the rolling temperature of workpiece, a thermocouple (type K) with 1.6mm in diameter was embedded in 50mm deep holes drilled at the tail ends of the specimen. The specimens were soaked at 1030°C for 1 hour to ensure a homogenous temperature distribution. When the center temperature of specimens reached 1000°C, the tests were conducted. For rolling the specimens with a diameter of 60mm, the roll was machined to have two oval grooves and a round groove as shown in Fig. 5.

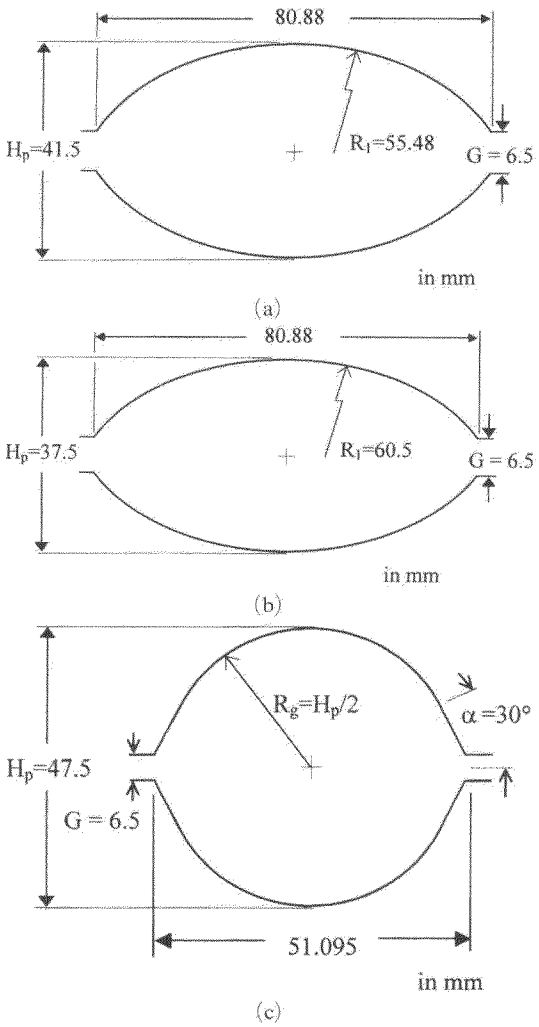

Fig. 5 Roll groove shape and design parameters for a two-pass rolling sequence (a) Oval(A) pass, (b) Oval (B) pass and (c) Round pass

The difference of the two types of oval grooves is the radius of curvature, R_1. A four-pass rolling sequence (Fig. 6) was also designed to roll the specimens with a 28mm diameter of 28mm.

A specimen was first rolled into the oval pass (Figs. 5(a) or 5(b)) at the desired temperature and cooled in air to room temperature. For the round pass rolling, the workpiece was re-heated up to the desired temperature in the furnace. The workpiece with an oval shape was then rolled into the round pass (Fig. 5(c)) after it was rotated through 90 degree about its length direction. Entry guides were installed in front of the roll groove to minimize sideway bending of specimen. After experiment, the cross sections with 30mm in thickness were obtained by cutting the middle part of workpiece in its length direction. Then, milling machine smoothed the cross section of workpiece. Finally, the coordinates of surface profile and cross sectional area were obtained by using the surface profile reading program followed by scanning the cross section of workpiece.

4. Results

Figures 7 through 10 illustrate the predicted surface profile of exit cross section and the experimentally obtained ones at the temperature of 1000°C with the rolling conditions (roll groove design, roll gap and specimen size) changed.

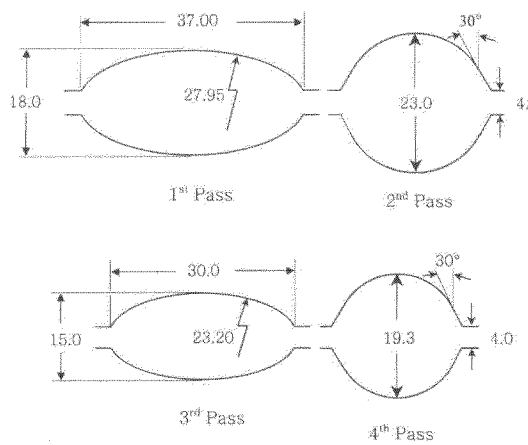

Fig. 6 Roll groove shape and design parameters for a four-pass rolling sequence

Figure 7 shows the predicted and measured cross sectional shape of workpiece at the oval pass and the round pass when the roll gap is 6.5mm. Dotted lines represent the roll groove shape. The cross sectional area measured at room temperature will inevitably be slightly smaller than the predicted one because the surface layers oxidized by air are scaled off after experiment. The predicted maximum spread and radius of surface profile exceed slightly the measured ones respectively. Figure 7(b) demonstrates that the incoming oval workpiece was somehow twisted along its length direction during rolling. Overall, the predicted cross sectional area is in good agreement with the measured one for both passes.

4.1 Effect of change of incoming size

Figure 8 illustrates that the maximum spread reaches almost the face width of oval groove when the specimen (66mm in diameter) is rolled. As expected, the increase of specimen diameter causes the maximum spread to increase. Overall, the predicted surface profile of workpiece is fairly in good agreement with the measured one regardless of the change of incoming specimen size. Figures 7 and 8 illustrate that differences between measured pass areas and predicted ones are in the range of 2.2~2.7%.

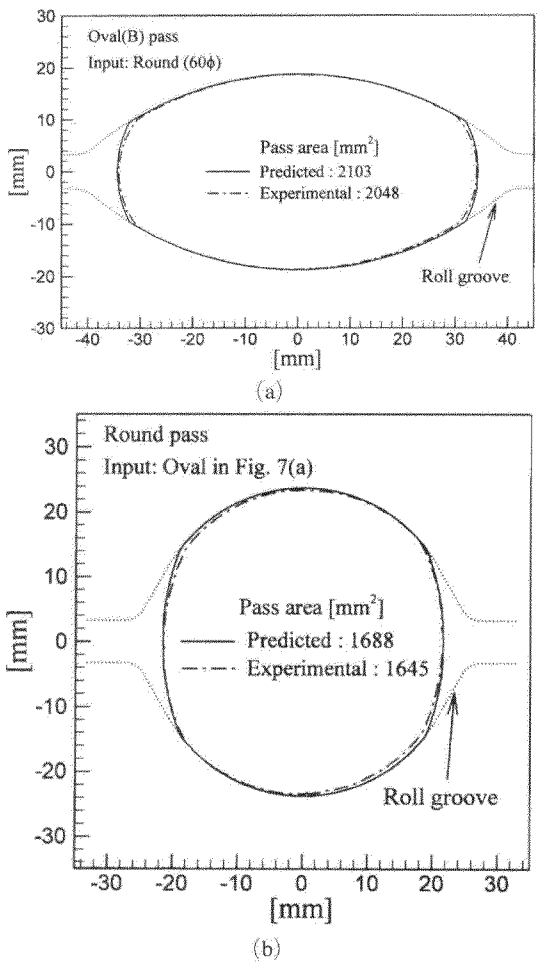

Fig. 7 Predicted and measured cross sectional shapes for the two-pass rolling (Fig. 5) when a specimen with 60mm in diameter is rolled

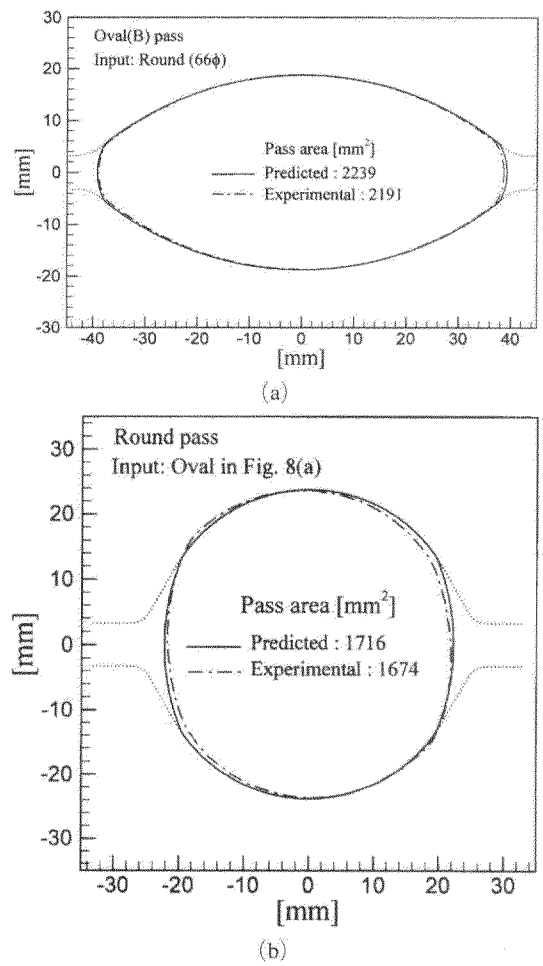

Fig. 8 Predicted and measured cross sectional shapes for the two-pass rolling (Fig. 5) when a specimen with 66mm in diameter is rolled

4.2 Roll gap change at oval pass

Figure 9(a) compares the experimentally measured cross sectional shape with the predicted one when the roll gap of the oval groove decreases to 2.5mm. It shows that the predicted maximum spread is larger than the measured one. Careful comparison of the oval groove profile with the experimentally measured cross sectional shape of deformed workpiece shows that the roll gap was slightly larger than 2.5mm during experiment. Hence, the height of workpiece became larger than the pass height, H_P, of the oval groove. Consequently, the measured maximum spread was smaller than the predicted one. Figure 9(b) shows that the calculated maximum spread is larger than the experimentally measured one. This is quite natural because the predicted maximum spread of the workpiece was already larger than that by experiment in the previous oval pass (Fig. 9(a)).

Comparison between the predicted surface profiles and measured ones is made in Fig. 10(a) when the roll gap of the oval roll groove is increased to 10.5mm. Good agreement is noted between the predicted surface profile and the measured one. In Fig. 10(b), the measured cross

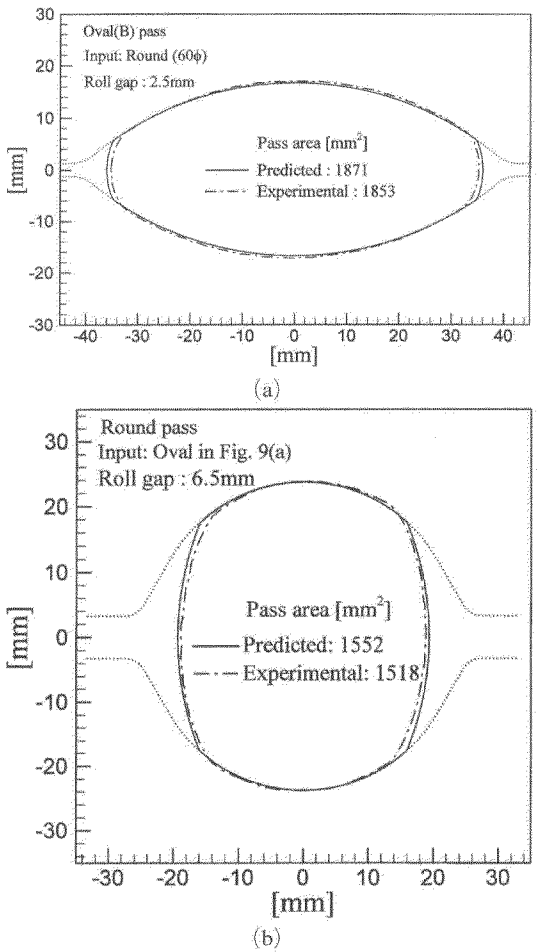

Fig. 9 Predicted and measured cross sectional shapes for the two-pass rolling (Fig. 5) when the roll gap of the oval pass was reduced to 2.5mm

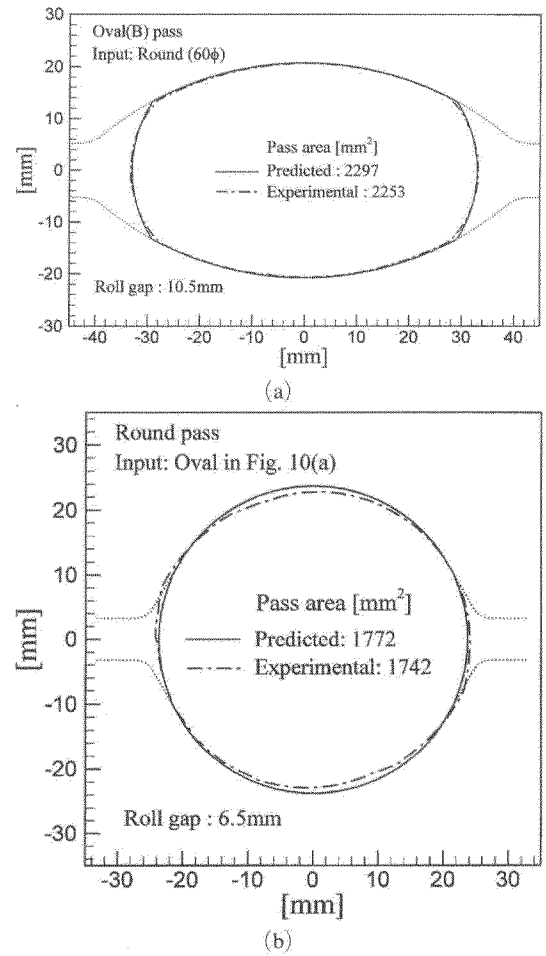

Fig. 10 Predicted and measured cross sectional shapes for the two-pass rolling (Fig. 5) when the roll gap of the oval pass was increased to 10.5mm

sectional shape does not look like a round shape in comparison with the predicted one, which is almost a round shape. It implies that the workpiece in the round groove has been twisted somehow along its length direction during rolling.

To check the twist problem of workpiece during rolling, a new entry guide is installed ahead of the round pass, which is able to prohibit rotation of workpiece during rolling. Figure 11 shows the predicted and experimentally measured cross sectional shapes when the new entry guide was installed. As can be seen, a nearly circular cross sectional shape was obtained from the experiment with the pass area unchanged. This result shows that the workpiece in Fig. 10(b) was twisted during rolling as expected and demonstrates the importance of entry guide especially ahead of round pass in rod (or bar) rolling process.

4.3 Change of design parameter of oval groove

The two types of oval grooves as shown in Fig. 5(a) and (b) were designed to investigate the effect of design parameter in oval pass rolling. Differences between oval(A) groove and oval(B) groove are the ratio of face width, W_f, to section height, H_p. Here, the ratio of W_f/H_p is defined as "aspect ratio" for convenience. Oval(A) groove in Fig. 5(a) has an aspect ratio of 1.95 and that of oval(B) groove in Fig. 5(b) is 2.16. For oval(A)-round pass rolling, the predicted and measured cross sectional shapes of workpiece were not compared directly. Instead, the radii of surface profile, R_S, and cross sectional areas of workpiece experi-

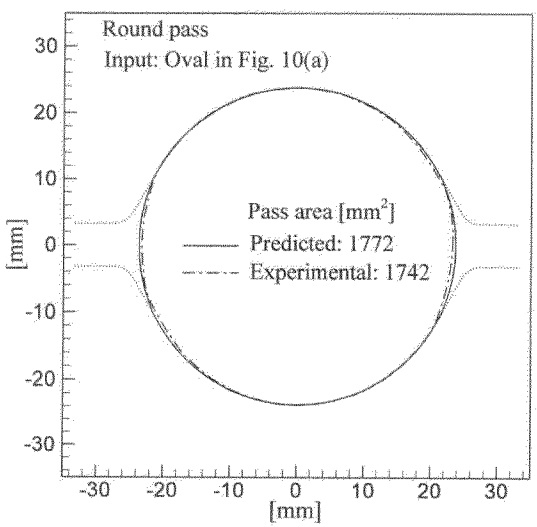

Fig. 11 Predicted and measured profiles of the exit cross section for the round pass rolling (Fig. 6(c)) when a new entry guide is used

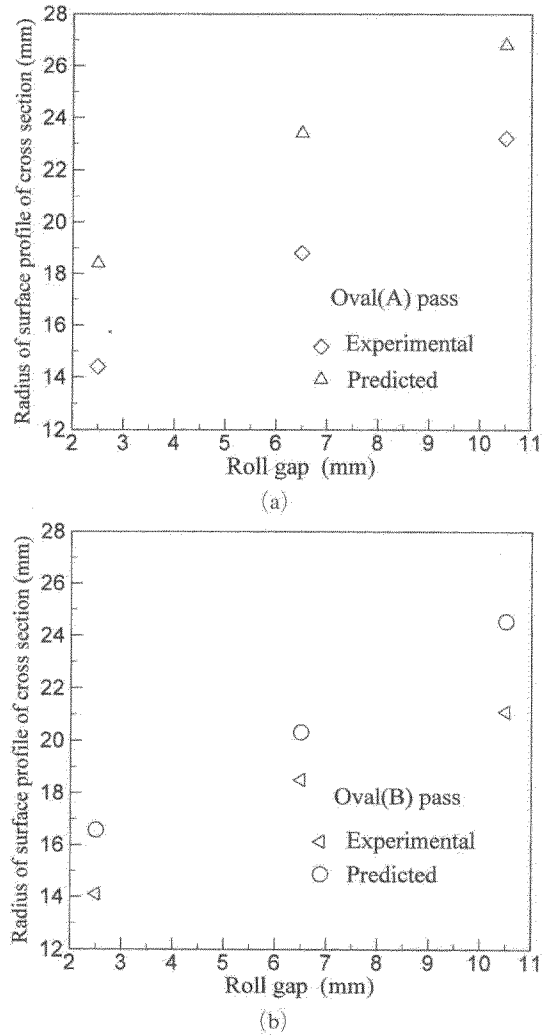

Fig. 12 Predicted and measured radii of surface profile for the two-pass rolling sequence (Fig. 5) when the roll gap of the oval groove is changed (a) oval(A) pass and (b) oval (B) pass

mentally measured and predicted are shown in Figs. 12 and 13.

In Fig. 12, the measured radii of surface profiles are compared with the predicted ones with the roll gap of the oval groove changed. The predicted radii of surface profile in oval(A) pass are always larger than those obtained experimentally. Meanwhile, in oval(B) pass, the differences between the radii of the predicted and measured surfaces profiles small.

Normalized cross sectional areas (A_{pred}/A_{expt}) of workpiece with changing the roll gap of the oval groove is illustrated in Fig. 13. In Fig. 13(a), a datum associated with roll gap of 10.5mm was left out because the test was invalidated due to overfilling at the round pass. The differences between the measured cross sectional area and predicted one are, respectively, in the range of 0.9~3.5% for the oval(B)-round pass rolling and −0.6~3.9% for the oval(A)-round pass rolling when the roll gap of the oval groove is changed up to ±61.5%. Therefore, we can deduce that the oval(B)-round pass sequence is better than the oval(A)-round pass sequence from the point of view of the pass sequence design.

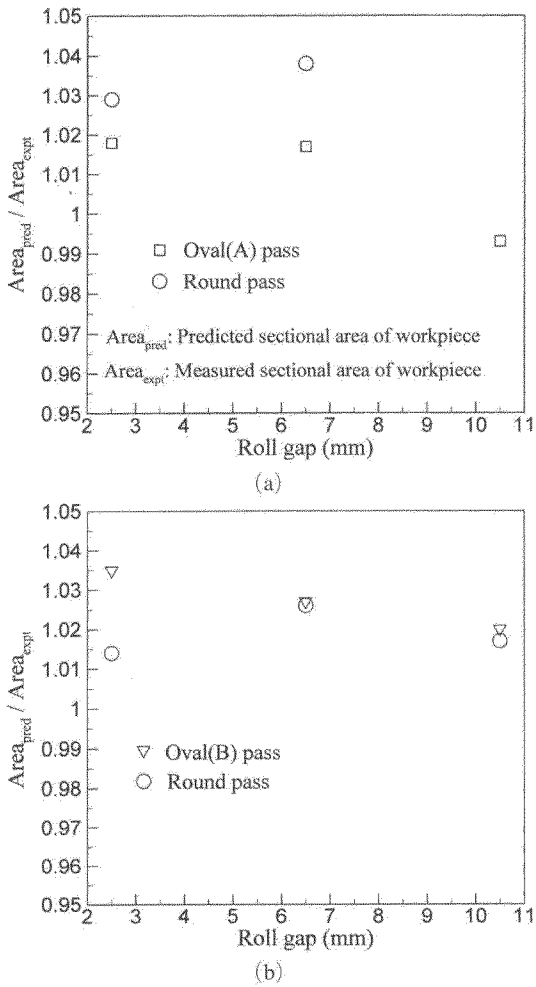

Fig. 13 Normalized cross sectional areas when the roll gap of the oval groove is changed. (a) Oval(A)-round pass sequence and (b) Oval(B)-round pass sequence described in Fig. 5

4.4 Change of the ratio of roll diameter to specimen diameter

To study the effect of the change of roll diameter to specimen diameter ratio on the model, we have designed a four-pass oval-round (or round-oval) pass sequence as shown in Fig. 6. The initial diameter of specimen is changed drastically, from 60mm to 28mm. The ratio of roll diameter to specimen diameter for the two-pass rolling sequence (Fig. 5) is 5.17(=310/60). Meanwhile, that of for the four-pass rolling sequence (Fig. 6) is 11.07(=310/28).

Figure 14 shows the predicted and measured cross sectional shapes/areas of workpiece for the four-pass rolling sequence. We can observe that at each pass at the first and third passes roll gap was set up slightly larger than expected. Overall, the cross sectional shapes/areas of workpiece predicted by the analytic model is in good concord with the measured one. It indicates that the analytic model is independent of the change of the ratio of roll diameter to specimen diameter.

4.5 Change of steel grades

In this section, an experimental study was carried out to investigate the effect of the change of steel grades on the exit cross sectional area. Figure 15 demonstrates that the dependency of the exit cross sectional area of the plain carbon steels and alloy steels over the temperature range of 800~1100°C, which is a typical temperature

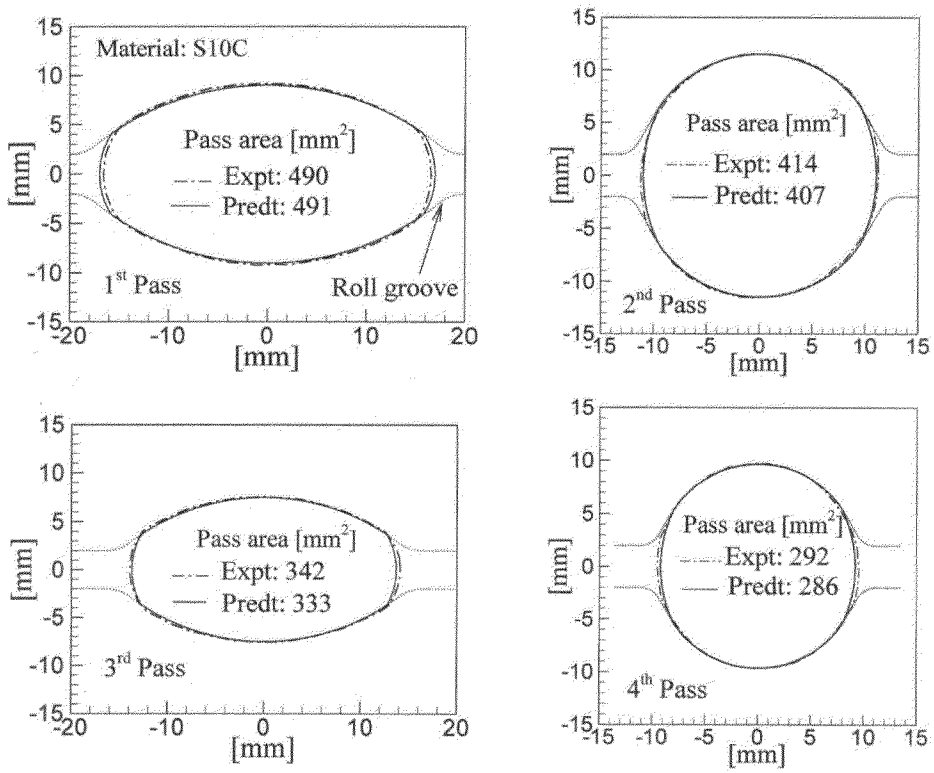

Fig. 14 Predicted and measured cross sectional shapes of workpiece for the four-pass rolling sequence as described in Fig. 6

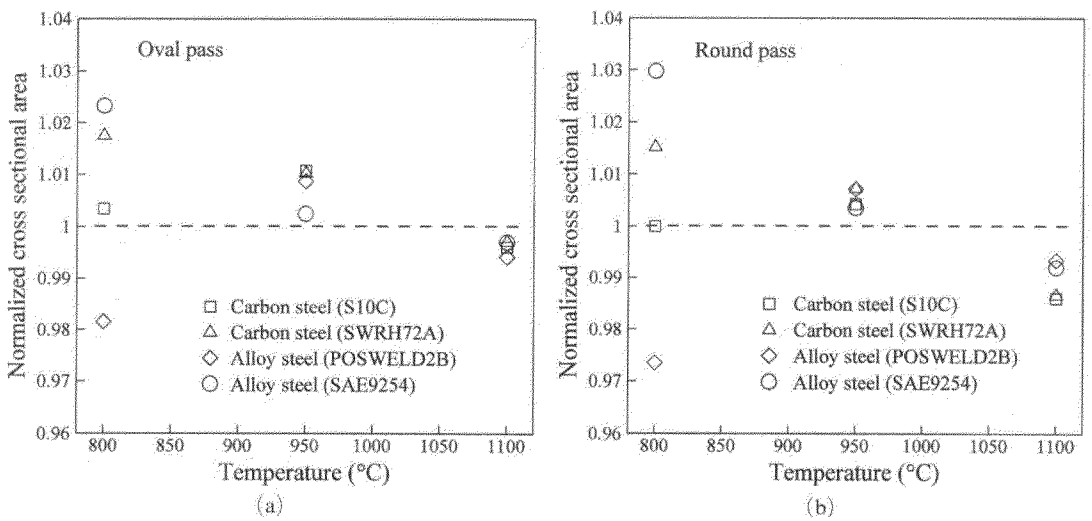

Fig. 15 Normalized cross sectional areas as a function of rolling temperature for plain carbon steels and alloy steels for the two-pass rolling sequence as described in Fig. 5(b) and 5(c)

range of the rod (or bar) rolling process producing those grade of steels. To normalize the cross sectional area, the cross sectional area (i.e., pass area) of those steel grades at each rolling temperature was divided by the one, which was rolled at the temperature of 1000°C.

The results show that the steel grades tested in hot bar rolling experiment influence little the cross sectional areas in the temperature range of 950~1100°C. However, when the temperature reaches 800°C, we can see the effect of steel grades on the pass area. In the case of POSWELD2B, the elongation is larger than that of the other steel grades. This is attributed to the microstructural characteristic of POSWELD2B. Meanwhile, the increment of pass area for the cases of SWRH72A and SAE9254 is due to the increased strength of the steels, which causes the roll gap (i.e., pass height) to increase. This was confirmed by measuring the pass height of the rolled specimens after experiment. The results presented so far have demonstrated that the spread correction coefficient γ in Eq. (1) is almost independent of the rolling temperature for the steels employed in this study, except POSWELD2B at around 800°C.

5. Discussion

The primary purpose of this study is to develop an analytic model for predicting the exit surface profile of workpiece in the oval-round (or round-oval) pass rolling sequence and demonstrate its generality, to see if the analytic model can be used for initial design of pass schedule and real-time control for rod rolling process.

The advantage of the developed model is that it requires only geometric considerations of roll groove and workpiece. Thus, the model greatly simplifies the problem of obtaining the final rolled shape only if the material is assumed to be incompressible during rolling and the maximum spread of the material interested of interest is obtained through a simple hot rod (or bar) rolling test. It should be noted that it is possible to predict the surface profile of workpiece in rod rolling by using three-dimensional finite element method. However, the accuracy of solution of it, in principal, still depends on the precise constitutive model of material at high temperature, which requires a lot of time and high cost for obtaining it. Thus, a lot of time can be saved if we use the proposed model in an initial design of the rolling schedule. In addition, the analytical model described in this study can be further extended to obtain an optimal design of rolling schedule, which typically requires very short computational time because of a tremendous number of iterations in computation.

The results obtained from this study demonstrated that the proposed model was of underlying experimental rationale to be used in rod (or bar) mills which have the oval-round (or round-oval) pass rolling sequence. Therefore, the analytic model can be industrially a very valuable tool. As a consequence, this work has established an important stage, advancing one step toward the on-line control of roll gap in rod (or bar) rolling process, which is aimed for obtaining good roundness of final rod (or bar) products with minimum variation.

Finally, as many people have aimed to transfer "Thermo-Mechanical Controlled Process (TMCP)" technologies for plate rolling to other hot rolling processes, this model may be a basis to assess the potential for developing TMCP technologies in rod (or bar) rolling because the model provides the key information (the cross sectional shape and area) which is necessary for computing the thermo-mechanical parameters such as the strain and strain rate at a given pass and the temperature variation across the cross section of workpiece during rolling and cooling between inter-stands (passes).

6. Concluding Remarks

In this study, an analytic model for the prediction of the exit cross sectional shape of workpiece during oval-round (or round oval) pass sequence was proposed. Then the validity of the model was examined by hot rod rolling experiment, with changing i) the initial diameter of specimen, ii) roll gap of the oval groove, iii) design parameter of the oval groove, iv) ratio of roll diameter to specimen diameter and v) steel grades. The conclusions are summarized as follows:

(1) The proposed model can be an effective tool for the initial design of rolling schedule and

optimization of rod (or bar) rolling process.

(2) The model described in this study may be further improved to predict the exit cross sectional shape when the roll gap of the round groove and rolling speed are changed, which is to be left as a future work because the rolling speed in field (rod mill) reaches as high as 50~100m/s and the roll gap of the round groove also varies.

References

Kemp, I. P., 1990, "Model of Deformation and Heat Transfer in Hot Rolling of Bar and Sections," *J. Ironmaking and Steelmaking*, Vol. 17, pp. 139~143.

Kim, N., Lee, S. M., Shin, W. and Shivpuri, R., 1992, "Simulation of Square-to-Oval Single Pass Rolling using a Computationally Effective Finite-Slab Element Method," *J. Eng. Ind.*, Vol. 114, pp. 329~335

Kim, S. H. and Im. Y. T., 1998, "Expert system for Roll Pass and Roll Profile Design for Shape Rolling of Round and Square Bars." *Trans. KSME (in Korean)*, Vol. 22, pp. 1781~1791.

Komori, K., 1997, "Simulation of Deformation and Temperature in Multi-Pass Caliber Rolling," *J. Mater. Proc. Tech.*, Vol. 71, pp. 329~336.

Kwon, H. C. and Im, Y. T, 1998, "Development of Interactive Computer Aided Design System for Roll Pass and Roll Profile Design in Bar rolling." *Trans. KSME (in Korean)*, Vol. 22, pp. 1336~1347.

Park, J. J. and Oh, S. I., 1990, "Application of Three Dimensional Finite Element Analysis to Shape Rolling Process," *J. Eng. Ind.*, Vol. 112, pp. 36~46

Shin, W., Lee, S. M., Shivpuri, R. and Altan, T., 1992, "Finite-Slab Element Investigation of Square-to-Round Multi-Pass Shape Rolling," *J. Mater. Proc. Tech.*, Vol. 33, pp. 141~154.

Shinokura, T. and Takai, T., 1983, "A New Method for Calculating Spread in Rod Rolling," *J. Applied Metalworking*, Vol. 2, pp. 175~188.

Wusatowski, Z., 1969, *Fundamentals of Rolling, Pergamon Press*, London, pp. 107~109.

Appendix

In Fig. A1, the equation describing the line O_1-B in x_1-y coordinate system is expressed as

$$y = a\, x_1 \tag{A1}$$

where

$$a = \frac{R_1 - H_p/2}{W_f/2 - R_f} \tag{A2}$$

An equation representing the upper part of oval groove can be expressed as

$$x_1^2 + y^2 = R_1^2 \tag{A3}$$

Substituting Eq. (A1) into (A3) yields y-coordinate of point B with origin of O_1

$$B_y = \left(\frac{R_1^2 a^2}{1+a^2} \right)^{1/2} \tag{A4}$$

The coordinate, B_y, can also be obtained from the geometric similarities

$$B_y = h + (R_1 - H_p/2) \tag{A5}$$

where

$$h = \frac{R_f (R_1 - H_p/2)}{R_1 - R_f}$$

The term 'h' in Eq. (A5) is derived from the geometric similarities of two triangles, $\Delta\, O_1\, O\, O_2$ and $\Delta\, B\, O_3\, O_2$, as

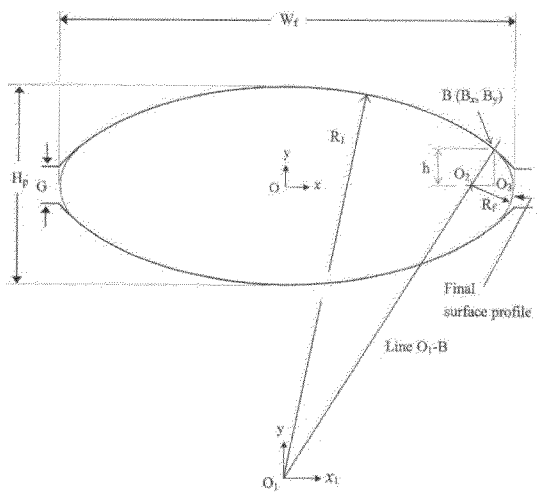

Fig. A1 Geometrical designation of oval groove and the radius of final surface profile, R_f, of a workpiece in the oval pass rolling

$$\frac{h}{R_f}=\frac{(R_1-H_p/2)}{R_1-R_f} \tag{A6}$$

Then, Eq. (A5) can be rewritten

$$B_y=(R_1-H_p/2)\left(\frac{R_1}{R_1-R_f}\right) \tag{A7}$$

Equating Eqs. (A4) and (A7) gives

$$\left[\frac{(R_1-H_p/2)^2}{a^2}\right]\left[\frac{R_1^2}{(R_1-R_f)^2}\right]=\frac{R_1^2}{1+a^2} \tag{A8}$$

Arrangement by using Eq. (A2) gives

$$\frac{(W_f/2-R_f)^2}{(R_1-R_f)^2}=\frac{1}{1+\left(\frac{R_1-H_p/2}{W_f/2-R_f}\right)^2} \tag{A9}$$

Rearranging Eq. (A9) yields

$$(W_f/2-R_f)^2+(R_1-H_p/2)^2=(R_1-R_f)^2 \tag{A10}$$

Thus, R_f can be expressed in terms of R_1, H_p and W_f

$$R_f=\frac{R_1H_p-\frac{1}{4}(W_f^2+H_p^2)}{2R_1-W_f} \tag{A11}$$